ORIGINAL ARTICLE

lajss.org© Latin American Journal of Solids and Structures

www.lajss.org

Seismic evaluation and partial retrofitting of concrete bridge bents with defect details

Mohammad Kazem Bahrani [a]

Amin Nooralizadeh [a*]

Nima Usefi [b]

Majid Zargaran [c]

[a] Department of Civil Engineering, University of Qom, Iran, Email: m.bahrani@iiees.ac.ir, aminnooralizadeh@stu.nit.ac.ir
[b] Centre for Infrastructure Engineering, Western Sydney University, Sydney, Australia, Email: N.usefi@westernsydney.edu.au
[c] Islamic Azad University Qazvin Branch, Qazvin, Iran, Email: Majidzargaran2011@gmail.com

* Corresponding author

https://doi.org/10.1590/1679-78255158

Abstract

The need for seismic retrofitting of bridges after severe earthquakes has become important in recent years. This study examines the seismic evaluation of concrete bents of highway bridges designed and implemented according to the 1990s regulations. Compared with the older codes, 1990s codes have more complex details for connections which are evaluated by experimental and numerical methods in this research. Significant improvement was observed in the behavior of the specimens designed with 1990s codes; however, this improvement is not enough as strength degradation was also reported in the inner cycles of the hysteresis curves. Therefore, seismic improvement was performed using performance levels. Results showed that in the connection zone, the longitudinal bar slippage occurs and the performance of connection is weak. In experimental phase, a specimen was constructed with external pre-stressing in a transverse direction for retrofitting. The level of improvement in behavior was also evaluated using parameters such as energy dissipation, performance levels and force-displacement curves.

Keywords

Cyclic loading, Seismic retrofit, Hysteresis behavior, Plastic hinge, Confinement

1 INTRODUCTION

Earthquake can cause severe damage in bridges which leads to many human casualties and financial losses. This issue has led to a global effort by researchers to improve the seismic performance of the bridges (Zadeh and Saiidi, 2007) by updating the seismic design codes. This is mainly because bridges designed by the old seismic codes were exposed to different types of damage in recent earthquakes in Japan, Turkey, United States, and Taiwan (Chen et al., 2005). Therefore, it is proven that the bridges designed by the old codes would have an inappropriate seismic performance in an earthquake. Different types of damage in a bridge under seismic loads can be categorized as follows: superstructure movement, lap splice failure, column bent damage due to shear and flexure, joint failure, abutment failure and unrecoverable damages that are due to insufficient lateral resistance, rapid strength degradation, and formation of plastic hinge at unintended locations (Hsu and Fu, 2004; Abe and Shimamura, 2012; Han et al., 2013; Kwon et al., 2011).

Received: June 28, 2019. In Revised Form: July 31, 2019. Accepted: August 14, 2019. Available online: August 19, 2019.
http://dx.doi.org/10.1590/1679-78255158

Concrete bridge with separate bent and superstructure is one of the most common highway bridges. In terms of design and technical specifications, several drawbacks are predictable such as flexural and shear weaknesses at bent members of the bridges causing a lot of damage to these bridges under earthquake load (Priestley et al., 1996). The existence of these defects in the design of column, cap beam and connection region have caused undesirable failure mode for these types of bridges under seismic loads. Thus, numerous studies have been carried out in recent years for estimating the type and extent of damage, determining the defects of column and connection region as well as new methods for seismic retrofitting of frames (Sritharan et al., 1999; Lowes et al., 2004; Vosooghi and Saiidi, 2013; Motaref et al., 2014; Javidan and Kim, 2019a; Noorsuhada et al., 2017).

According to numerical studies and initial calculations, Priestley et al. (1993) showed that the San Francisco double-deck viaducts were not suitable for the desired seismic performance level. The columns, cap beams and connection regions of the bridges do not show good performance when designed based on capacity-based design method. In their study, a ½ scale experimental specimen, according to the status quo of the bridges, was subjected to cyclic loading and they presented a new method for retrofit of bridges based on the results. Among the studies conducted to investigate and identify the defects and problems of bridges constructed before the 1970s, experimental studies of Sritharan et al. (2001) have been of great importance. In this study, the current seismic design was evaluated by comparing some multi-column concrete bridges with the cap beam. A large number of existing bridges in the United States, subjected to California's past earthquakes (San Fernando and Northwest Territories earthquakes) which faced a lot of damages can be a justification for these studies.

Tehrani and Mitchell (2013) have conducted a study on seismic risk evaluation on 15 four-span bridges, designed according to Canadian 2006 codes. The specimens with different columns heights and diameters were subjected to incremental dynamic analysis (IDA). Some factors such as bar slippage, loss of concrete cover, buckling of bar and collapse of the structure were predicted in their study. By comparing the results of this research, the defects and problems of the old codes can be well understood. Recently, fragility analysis has been used on several multi-column retrofitted bridges designed by the old seismic codes to estimate their vulnerability to seismic loads. This method estimates the damage of bridges after an earthquake (Billah et al., 2012).

In this study, two 30%-scale concrete bents from a double-span bridge were designed based on the 1990s codes (Caltrans, 1994) and New Zealand Standard (NZS) (NZS, 1995) and subjected to cyclic loading. While the first specimen (specimen A) was based on built conditions, in the second specimen (specimen B) external transverse pre-stressing stirrups were used on cap beams for rehabilitating of the specimen. The seismic behavior of the specimens was evaluated, analyzed and compared with the similar specimens designed based on the 1980s codes that were previously studied by Bahrani et al. (2017). The study aims to determine if the details of the new codes (1990s codes) are sufficient to improve the seismic behavior of the bridge or the need for retrofitting is still considerable. It is also of great importance to evaluate the need for rehabilitating of connections and optimize this process.

Moreover, the study by Bahrani et al. (2017) showed that the actual behavior of a multi-column bridge and its retrofitted specimen especially in connection regions under seismic loads could be predicted well with a numerical approach. The effect of bar slippage under lateral loads was also considered with materials available for steel bars and zero-length elements. This study aims to evaluate the seismic behavior of a bridge frame, designed based on the 1990s codes, and compare the results with the same bridge designed by 80s codes.

2 COMPARISON OF SOME COMMON CODES IN DIFFERENT YEARS

Three codes of United State, New Zealand and Japan are presented in different years in Table 1 for better evaluation of the type of damage and design of the connection region. These requirements include limitations in shear stresses, requirements for connection reinforcement, confinement and number of bars (Naito et al., 2001).

Table 1: Common Different Codes for Connection Region.

Country	Code	Reference
United States	ACI 352, ASCE-ACI Joint Committee	(ACI 352, 1983)
United States	California Department of Transportation, Bridge Design Specification	(Caltrans, 1994)
United States	Applied Technology Council Recommendation (ATC)	(ATC, 1996)
New Zealand	Standard 3101- Code Practice for the Design of Concrete Structures	(NZS, 1982)
New Zealand	Standard 3101- Code Practice for the Design of Concrete Structures	(NZS, 1995)
Japan	Architectural Institute of Japan — Structural Design Guidelines for Reinforced Concrete Buildings	(AIJ, 1994)

2.1 Shear stress limitations

Some limitations are applied to the amount of stress at joint to make sure that beam-column connection can withstand plastic hinge mechanism. A study in Japan showed that the shear strength of joint strongly depends on compressive strength of concrete and on transverse bars in the hinge (Kitayama et al., 1991). Fig. 1 shows the relationship between the allowable shear strength and the compressive strength of concrete in different codes. Accordingly, the compressive strength of concrete is one of the important parameters for determining the shear strength of the connection (Naito et al., 2001).

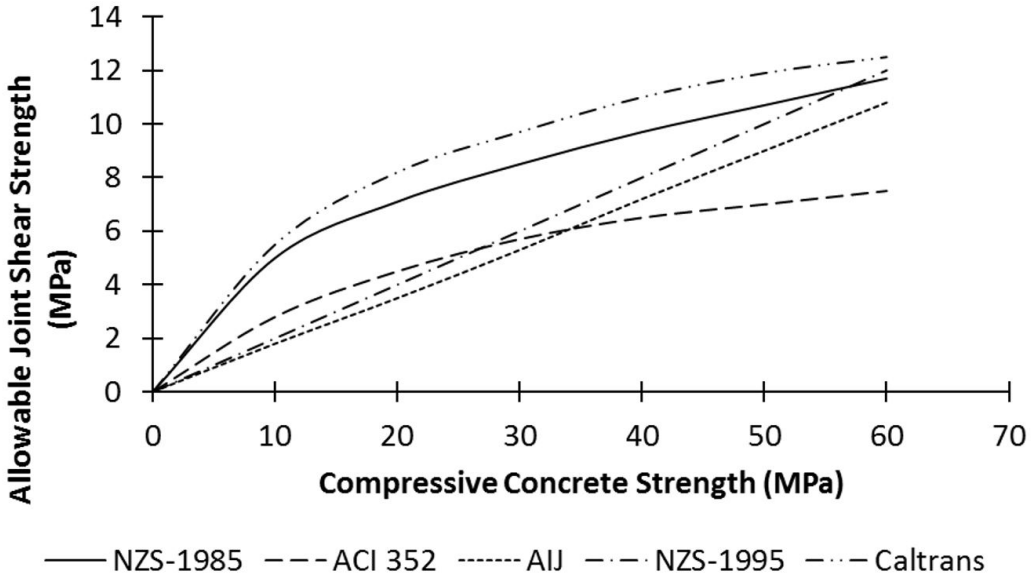

Figure 1: Shear stress limitations for interior joints by different Codes (Naito et al., 2001).

2.2 Requirements for design of connection reinforcement

The reinforcement in connection region is usually determined according to the connection demand level. Hence, this level of demand is assigned by codes in two categories: first, the demand level that is due to shear in connection region; and second, the demand level that is due to tensile force in tensile members in the connection region. Therefore, the joint capacity depends on the strength of the bars and number of them in the connection region. The approaches used by each code for obtaining the demand level are summarized in Table 2 (ACI 352, 1983; NZS, 1982; NZS, 1995; Caltrans, 1994; AIJ, 1994; ATC, 1996).

Table 2: Joint Reinforcement Requirements.

Design Code	Requirements
NZS 3101 (1982)	Joint reinforcements are needed for horizontal and vertical joint. Reinforcement positioned between the outer layers of beam longitudinal bars. Column bars or additional vertical stirrups which are hooked into the section can be counted as vertical reinforcement.
ACI 352 (1983)	Column ties or spiral which are horizontal transverse reinforcement, are necessary for joint confinement and this is not affiliated with joint shear.
Caltrans (1994)	Both horizontal and vertical transverse reinforcement are needed in location of the joint. Cap stirrups and additional bars hooked around the longitudinal reinforcement should be comprised by vertical transverse reinforcement. Horizontal reinforcement includes hairpins jointed into the beam in two or more layers with a higher density outside the column core.
AIJ (1994)	If a beam plastic hinge forms, horizontal transverse reinforcement is needed. Vertical transverse reinforcement is necessary when there is a column plastic hinge. The amount of reinforcement depends on the shear force. Transverse reinforcement is enough for one direction.
NZS 3101 (1995)	Based on the new information regarding the effect of concrete and steel strength to bond capacity in the joint core, the amount of horizontal transverse reinforcement can be reduced. Joint reinforcement in one direction is a function of the other direction.
ATC 32 (1996)	The amount of column longitudinal reinforcement developed into the joint specifies the quantity of vertical transverse reinforcement

2.3 Investigation of confinement

By increasing the confinement of members at connection region, the reinforcement needed can be reduced. Therefore, some codes have considered this reduction in number of bars due to the confinement at connection region. Based on both NZS 3101 (1982) and NZS 3101 (1995) codes, it is possible to reduce the shear reinforcement of the connection if the cap beam is elastic. The reduction in horizontal bars is also allowable in ACI 352 (1983) and AIJ (1994). This reduction is allowable neither in the Caltrans (1994) nor in ATC 32 (1996) codes.

2.4 Reinforcement in the connection region

Table 3 shows the summary of the allowable reinforcements in different codes at the connection region. The section dimensions are considered constant in all cases to have a better comparison. The requirements in these codes vary considerably. For example, ACI 352 (1983), AIJ (1994), Caltrans (1994), and NZS (1995) consider the transvers reinforcement from 0.2% to 0.5%. In ACI 352 (1983), it is recommended that column transverse reinforcement continue through the joint; whereas in Japanese code (AIJ, 1994) it is mentioned that the transverse reinforcement should be continued from the stronger member. The required reinforcement in both Caltrans (1994) and NZS (1995) is similar and the moderate reinforcement for joint is about 0.3%.

Table 3. Connection Reinforcement Requirements (Naito et al., 2001)

Specification	Vertical transverse reinforcement ratio	Horizontal transverse reinforcement ratio (spiral)	Horizontal transverse reinforcement ratio (straight bars)	Total volumetric transverse reinforcement ratio
ACI 352 (1983)	0	0.203%	0	0.203%
AIJ (1994)	0.109%	0	0.108%	0.217%
Caltrans (1994)	0.129%	0.085%	0.125%	0.339%
NZS 3101 (1982)	0.316%	0.092%	0.125%	0.533%
NZS 3101 (1995)	0.102%	0.095%	0.125%	0.322%
ATC 32 (1996)	0.473%	2.500%	0.092%	3.065%

2.5 Plastic hinge

Connection demand is governed by the formation of plastic hinges in adjoining beams for designing the beam column connection. Formation of the plastic hinge in beams of the bridge is either undesirable or unattainable. For instance, in single-column bents, plastic hinges form only within the bottom of the column under lateral loading, plastic hinges can be expanded along the beam in multi-column bridge bents with integral box girders. However, due to the problem of limited access to the beam region for post-earthquake repair and inspection, this mechanism is uneconomical. Development of a beam plastic mechanism in multi-column bridge bents supporting concrete or steel girders can result in the overthrow of the girders deformation in the bridge deck. Due to the above-mentioned problems and even the safety sides, plastic hinge formation is positioned in the columns where repair and inspection are easily handled (Fakharifar et al., 2015).

For bridge systems, the superstructure relative weight is low and P-delta effects are usually not adequate to cause progressive collapse (Shayanfar and Javidan, 2017; Javidan and Kim, 2019b, Mohajeri Nav et al., 2018). As deformability of bridge column is always high, reinforcement detailing in common design methods is based on having hinges in column directly below the cap beam or above footing. Based on NZS (1995) and AIJ (1994), levels of joint reinforcement are relative to the member which plastic hinge forms whereas ACI 352 (1983) and Caltrans (1994) implicitly assume that formation of plastic hinge occurs in the beam and column, respectively (Naito et al., 2001).

2.6 Shear in the connection zone

Due to the importance of connection shear force, the beam-column connection is of great importance in reinforced concrete frame design (Hosseini et al., 2019a; Ahmadi et al., 2016; Javidan et al. 2018; Hosseini et al., 2019b). Several cases of connection shear-failure of outrigger bent-knee joints occurred in the Loma Prieta earthquake. One example of the cap beam flexural-shear failure can be seen in Fig. 2. This connection failure is accompanied by diagonal crack propagating from the outside top corner of the joint. Diagonal shear cracks are developed corresponding to both opening and closing connection moments. Many codes have considered requirements for connection reinforcement to ensure satisfactory performance and safety under seismic loading.

Another example of knee-connection shear failure, damaged in the Loma Prieta earthquake in Oakland California, is shown in Fig. 3. This bridge was designed and constructed based on the 1980s codes with several undesirable features. Connection reinforcement consisted of very light transverse spirals, which had the capacity to resist less than 10% of horizontal connection shear force (Priestley et al., 1996).

Figure 2: Cap beam flexural-shear failure (Priestley et al., 1996).

Figure 3: Knee-joint shear failure of connector damaged in the Loma Prieta earthquake (Priestley et al., 1996).

3 SPECIMEN DESIGNED BASED ON 90s CODE

The specimen A is a representative of the design based on 90s codes. The most important difference between this specimen and the one designed with 80s code is the increase of transverse reinforcement in connection region with no differences in the number and diameter of longitudinal reinforcements. The issue of longitudinal reinforcement anchorage in column at the connection region has been solved compared to the previous codes. However, it is necessary to evaluate if the conditions for seismic behavior are sufficient or the need for seismic rehabilitating should be further investigated. This study evaluates the seismic behavior of a bridge frame, designed based on the 1990s codes, and compares the results with the same bridge designed by 80s codes as discussed by Bahrani et al. (2017). In addition, another specimen (specimen B) as a retrofitted specimen was also evaluated in this study. In previous study by Bahrani et al. (2017), the retrofitting was based on an external pre-stressing in two directions, whereas in this study the retrofitting was in transverse direction with same external pre-stressing. In general, the differences of specimens based on the 1980s and 90s codes are as follows:

The specimen which is designed based on the 90s codes is similar to 80s codes in terms of the physical geometry conditions, cross-sections, dimensions and sizes. However, the stirrup spacing in column height was designed by the AASHTO (2007) regulation for the regions of plastic hinge and extended to half of the longitudinal bar development length in the connection region. However, this extension of the stirrups is not considered in 80s codes. These details are often used by current design codes and are now more in use. In this study, the ratio of the longitudinal and transverse reinforcements and the dimensions of the specimens have been considered and implemented based on averaging of values of the similar common bridges (six bridges).

The scale of the experimental specimen was considered as 30% of average values of six present bridges. Specification of materials was selected based on field studies and available test results. For concrete, the strength of the standard cylindrical specimen was 24 MPa and compressive strength of the cap beam and column were 28.6 MPa and 27.5 MPa, respectively. The details of the longitudinal and transverse reinforcements are presented in Table 4. A general comparison between specimens designed by 80s codes, as stated by Bahrani et al., (2017), and 90s codes is also shown in Table 5. As is seen, there are no differences between the two models in terms of type, size and strength of reinforcement. The major difference is the spacing of transverse reinforcements, which is reducing this value especially in the connection region, as presented in the 90s codes, causes better seismic behavior for bridge. Specimen B that is also a retrofitted type of specimen A was strengthened by transverse pre-stressing in the external connection region. Specimen A and B are shown in Figs. 4 and 5, respectively. For better understanding of the retrofitting in specimen B, details of pre-stressing are also shown in Fig. 6.

Figure 4: Specimen designed based on 90s code (specimen A).

Figure 5: Retrofitted specimen with one side external pre-stressing (specimen B).

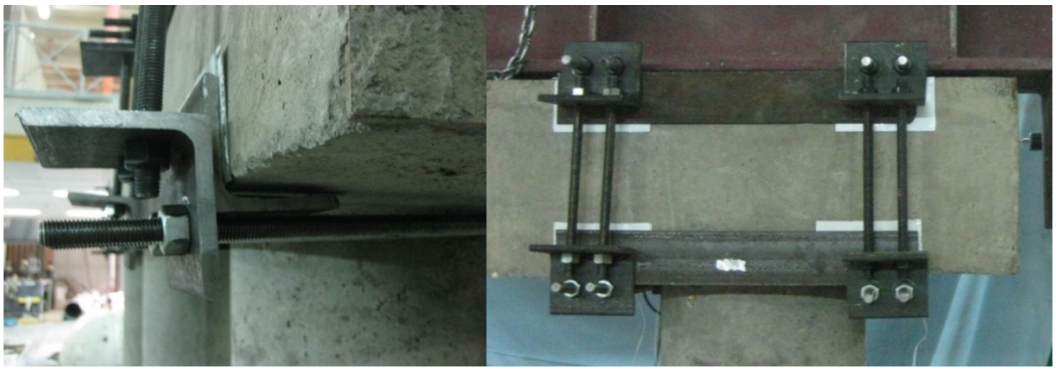

Figure 6: Details of steel jacket for specimen B.

The external confinement strain can be calculated based on the equation proposed by Mander et al. (1988). The direct effect of external stress on the bond stress of concrete and steel and the improvement of confinement is considerable. However, this effect depends on the conditions of applying external stress and the measurement method. Untrauer and Henry (1965) showed that the bond stress of concrete and steel is related to the root of external stress. Hence, they proposed a relationship for the start of the bar slippage. In the absence of confining transverse reinforcement, the external stress (f_p) can be applied to the bar development length (l_a). Therefore, with the assumption of the contribution of the 50% lateral stress for the anchorage of the reinforcement, the following relation is gained which f_y and d_b are the yield stress and diameter of the bar, respectively.

$$0.5\,A_b f_y = 0.5\mu P_b l_a f_p \;\rightarrow\; \pi d_b{}^2 f_y = \mu\,\pi d_b l_a f_p$$
$$f_p = d_b f_y \,/\, \mu l_a \tag{1}$$

$$f_p = \frac{d_b f_y}{1.4\times 25 d_b} = 0.028 f_y \tag{2}$$

It can be easily shown for bar development length equal to 25 times of the diameter of the longitudinal bar ($l_a = 25 d_b$) and the friction coefficient equal to $\mu = 1.4$, the confining transverse stress becomes equal to $f_p = 0.028 f_y$. This value for steel with a yield stress of 400 MPA and the compressive strength of concrete $f_c' = 24MPa$ is approximately $f_p = 0.48 f_c'$ and applying this level of transverse stress is relatively difficult. Therefore, according to Priestley et al. (1996), by applying a base stress around $f_p = 0.05 f_c'$ a successful and effective design can be gained. This design improves the problem of longitudinal reinforcement anchorage in the

connection region. For specimen B, the same base axial stress (0.05f'c) was applied to the left connection and twice of this value was used for the right connection.

Table 4: Mechanical Properties of the Transverse and Longitudinal Bars Used in Specimens.

Type of bar	Yield stress F_y (MPa)	Ultimate stress F_u (MPa)	Ultimate strain $\varepsilon_u(\%)$
Longitudinal	503.4	671.3	12.92
Transverse	348.3	538.2	12.47

Table 5: Comparison of Specimen Details Based on 1980s and 90s codes.

Specimen designed by 90s code	Specimen designed by 80s code		
350	350	Cross section diameter (mm)	**Details of the column**
2500	2500	Free height (mm)	
1200	1200	Spacing between columns(mm)	
16T10	16T10	Longitudinal reinforcement	
10	10	Diameter of bars (mm)	
16	16	Number of bars	
1.31	1.31	Percentage of bars *(%)*	
T8@50	T8@60	Transverse reinforcement of hinge region	
Spiral	Spiral	Type	
8	8	Diameter (mm)	
50	60	Spacing (mm)	
0.29	0.24	Percentage *(%)*	
T8@50	T8@60	Shear reinforcement	
8	8	Diameter (mm)	
50	60	Spacing (mm)	
0.24	0.24	Percentage *(%)*	
300	300	Section height (mm)	**Details of the header**
500	500	Section width (mm)	
6T10	6T10	Upper reinforcement	
10	10	Diameter (mm)	
6	6	Number	
0.31	0.31	Percentage *(%)*	
4T10	4T10	Lower reinforcement	
10	10	Diameter (mm)	
4	4	Number	
0.21	0.21	Percentage *(%)*	
2T8@100	2.25T8@100	Transverse reinforcement	
8	8	Diameter (mm)	
100	100	Spacing (mm)	
2	2.25	Number	
0.20	0.23	Percentage *(%)*	
T8@50	T8@150	Confining reinforcement	**Details of the connection region**
200	150	Length (mm)	
8	8	Diameter (mm)	
50	150	Spacing (mm)	
1.15	0.38	Percentage *(%)*	
240	240	Bar development length of column	

4 TEST SETUP

The test setup and components used to install the experimental specimen and rigid floor are shown in Fig. 7. This setup was based on the study of Bahrani et al., (2017) to have a good comparison between the results of this study and the previous one. According to the lateral loading pattern, the zero moment region is located at the midpoint of the column height. Hence, it is possible to assume simple joint in the middle of the column. Therefore, with modelling of upper part of the concrete frame, the bottom end of the columns is considered as a hinge (Flores, 2004). The connection of concrete columns to the base steel beams of the test frame was done with high-strength bolts to allow rotation and to provide hinge boundary conditions. Gravity load was applied with the use of high-strength bolts symmetrically placed on the sides of the test specimen, between the upper and lower steel beam. After placing the specimen and placing the transverse beam on the elastomers and on the specimen, the gravity load was applied to the concrete frame by tightening the side bolts.

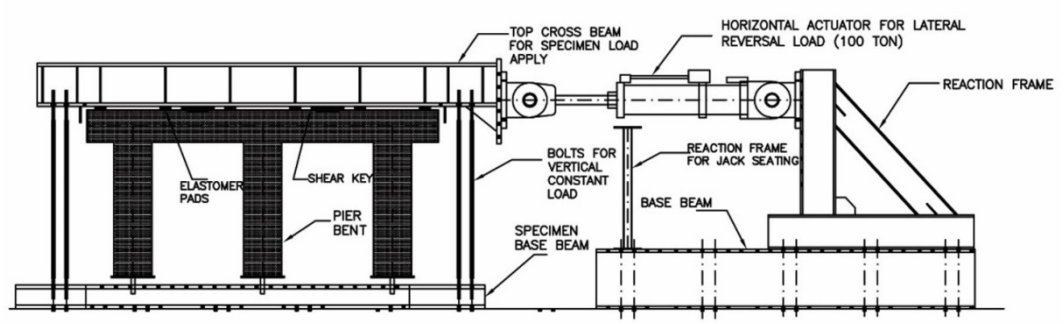

Figure 7: Details of the test setup.

During the experiment, the bolts strains were measured using strain gauges and elastomers stiffness was selected so that the stress in the bolts during the lateral displacement of the concrete frame was negligible. The 500 KN axial load was applied to the specimen through bolts. The lateral load on the real bridges was transferred to the concrete frame by means of shear studs, located on cap-beam. A cyclic loading, with specified protocol ATC (1992) was applied to the specimen up until the strength degradation and ultimate failure of the specimen.

5 FINITE ELEMENT MODELLING

The purpose of numerical modelling is to provide a fairly accurate evaluation of the damage and performance of structures (Usefi et al., 2019; Liu et al., 2014). The study used a nonlinear macro method based on the definition of fibre elements in OpenSees software due to the importance of hysteresis behavior of the concrete frame. The proposed model in this study can predict the bar slippage at the connection region under cyclic loading. Many studies have been carried out to evaluate the bond slip between steel and concrete to predict the force-slip deformation relationship. These studies are based on strong experimental research to predict the backbone curve of force-slippage in uniform and non-uniform bond stresses (Otani and Sozen, 1972; Morita and Kaku, 1984; Saatcioglu et al., 1992; Sezen and Moehle, 2003). The weakness of these studies was the inability to predict bond slip in cyclic loads. Therefore, many efforts have been made by researchers to predict the bond slip in RC members under cyclic loading and some relationships were gained by pull out test (Hawkins et al., 1987; Pochanart and Harmon, 1989; Soroushian and Choi, 1989). Bond stress between concrete and bar under cyclic loads, especially in the connection regions of the column to cap beam, has been highly regarded by the researchers due to its effect on the seismic behavior of the frame. Several studies have led to the development of relatively precise relationships such as the Zero length element proposed by Zhao and Sritharan (2007) or the model for steel bars proposed by Dodd and Restrepo-Posada (1995), as well as the combination of these two relationships to predict the retrofitted frame behavior (Bahrani et al., 2017). Both above-mentioned proposed models were used in this study. The relationships of Priestley and Paulay (1992) were used for applying the properties of confinement concrete in column core, too. In the retrofitted specimen, the retrofit design was implemented by using transverse pre-stressed jackets in external connections. Their performance should be simulated in the modelling to simulate these metal jackets in numerical modelling. Concrete01 material was used for confined and unconfined concrete, and confined concrete stress was calculated based on existed relationships available in the study of Bahrani et al. (2017). Equation 3 was used to calculate the confining strain in the retrofitted specimen model in which f'_{cc}: is the compressive stress of confined concrete, f'_{co} and ε_{co}: are compressive stress and

strain of unconfined concrete and ε_{cc} is the strain of unconfined concrete (Mander et al., 1988). ε_{co} is assumed to be 0.002 . Fig 8a. shows the simplified model of experimental specimens in OpenSees. As it can be seen in Fig 8b, the bond slip effect is considered by a bond slip material in OpenSees.

$$\varepsilon_{cc} = \varepsilon_{co} \times (1 + 5(\frac{f'_{cc}}{f'_{co}} - 1)) \tag{3}$$

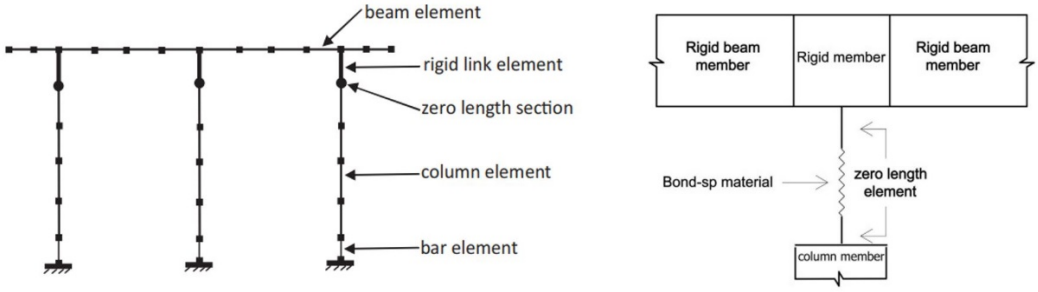

a) Simplified model of specimen b) Modelling of bond slip in OpenSees

Figure 8: Numerical modelling schematic

6 RESULTS

6.1 Hysteresis curves

This section presents and compares the hysteresis behavior of the experimental specimens with the numerical method. Concrete frames were subjected to cyclic loading up until the ultimate capacity of the bars and complete failure of the concrete core were seen. Fig. 9 shows the experimental and numerical hysteresis behavior of the specimens A and B.

Hysteresis curves of the specimens designed by older codes, show significant in-cycle and out-cycle strength degradation and little plastic behavior by entering the nonlinear range (Bahrani et al., 2017). For determination of the ductility, the behavior and performance of the specimen and damage progression pattern should also be considered. In terms of energy absorption and damping, the hysteresis curve is thin and its energy absorption is negligible due to the slip of longitudinal reinforcement. The hysteresis curve of the specimen A (Fig 9a) shows high and low in-cycle and out-cycle strength degradation, respectively, by entering to the nonlinear range. This in-cycle strength degradation can be attributed to the slippage of the bars. Due to the lack of formation of a desirable mechanism in the members, the hysteresis curve is thin and does not have high energy-absorption. Fig. 9b shows the hysteresis curve of specimen B with slight strength degradation. This specimen also has a lower pinching behavior, which indicates a decrease in the bar slippage in the connection region compared to the other specimen. Improving the seismic behavior of the specimen A and B compared with the specimens designed with older codes is clear from the results. In addition, the specimen B showed better behavior compared to the specimen A. The envelope curves of the specimens are extracted and illustrated on Fig. 10 for a better comparison between the results.

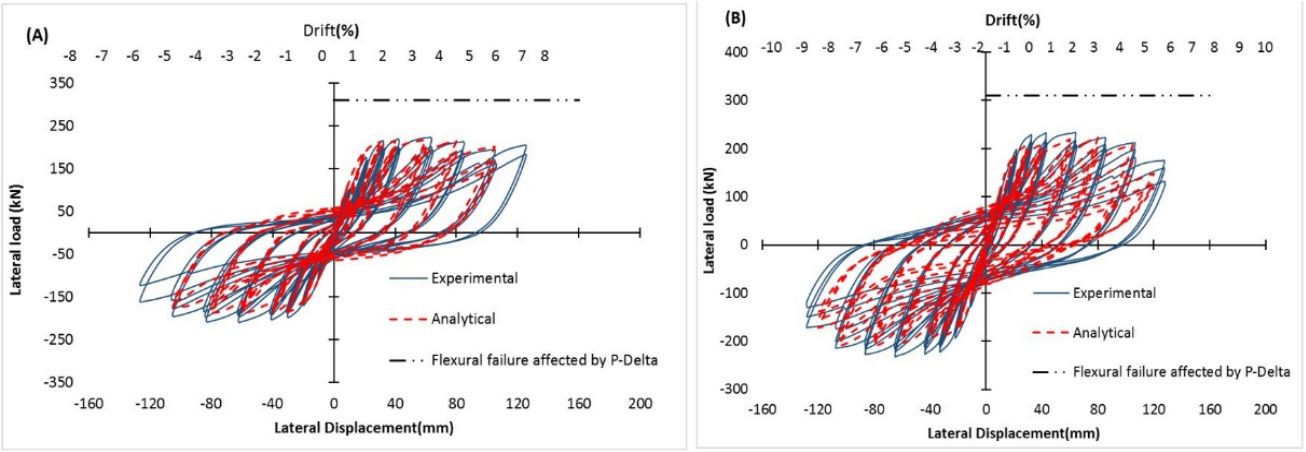

Figure 9: Experimental and numerical hysteresis results of the specimens designed by 1990s codes. a) Specimen A b) Specimen B

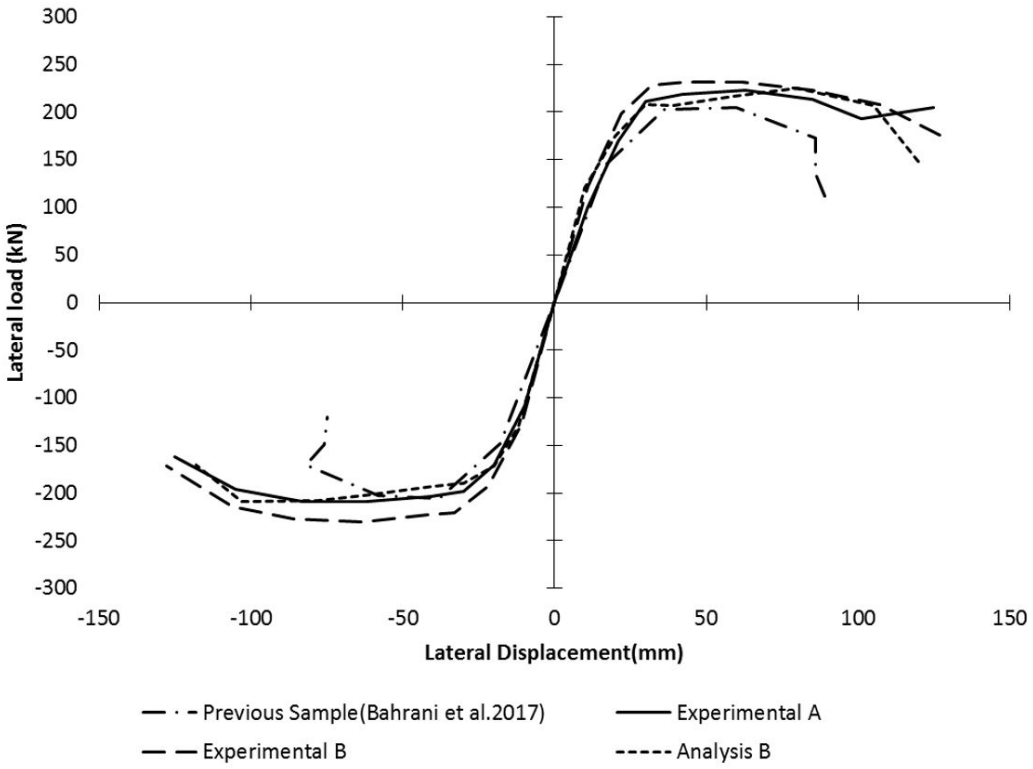

Figure 10: Envelope curve of the specimens.

6.2 Strength degradation process

The percentage of strength degradation is defined as the difference between loads resisted in the two cycles divided by the load resisted in the first cycle of that pair of cycles for that displacement amplitude. Overall, specimen B showed low-strength degradation. The strength degradation index to the relative displacement is shown in Fig 11. Relative displacement is calculated by dividing the structural displacement on the ideal displacement. Up until the relative displacement of 1, less than 2% of the strength degradation between the first and second cycles in particular displacement amplitude was observed in specimens A and B as is seen in Fig. 11a. At this relative displacement, strength degradation in the second and third cycles was neglected (less than 1%) based on Fig. 11b. For specimen A, the first cracks appeared in relative displacement of 0.5 as flexural capillary cracks in cap beam, whereas the flexural cracks in the specimen B appeared at a relative deformation of 0.7. The behavior of the specimens at this displacement range only leads to the formation of capillary cracks on the concrete surface. For specimen A, the strength degradation of cap beam was strongly influenced by loading in relative deformation of 1. For the specimen B and at relative displacement of 1.5, the cracks caused by the bar confinement first appeared in the left connection and then in the middle and right side connections, as seen in Fig. 11a.

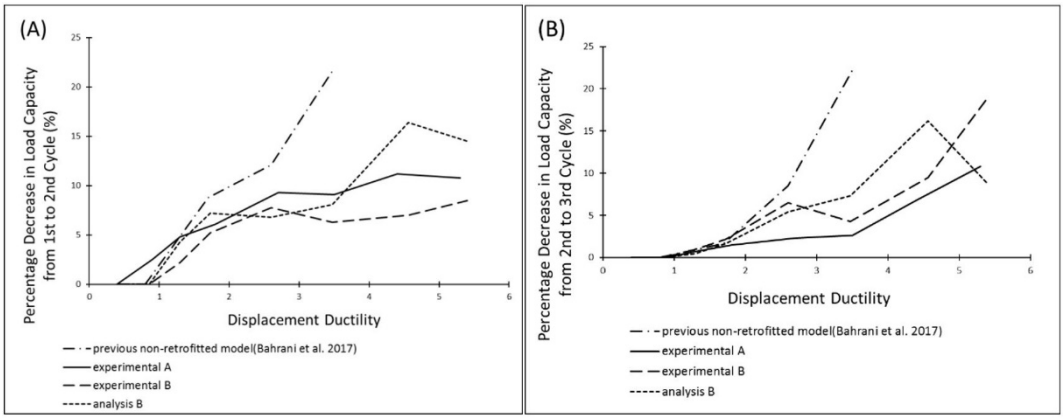

Figure 11: Experimental and numerical results of the strength degradation of all specimens

a) Between first and second cycles b) Between second and third cycles.

For specimen B, in relative displacement above 2.2, simultaneously with increasing the width of the columns cracks, the concrete cold joint crack also began to progress in the connection region. However, in specimen A, before the relative displacement of 1.3, the vertical cracks caused by bar slippage in connection region were appeared and propagated up until the relative deformation of 2. The cracks increased at this stage up until they propagated all over the section and concrete cold joint crack appeared at connection region. At this stage, due to moderate displacement, the concrete cracks and the bar slippage increased.

There is a significant difference between the strength degradation in the second and third cycles at the relative displacement ranges of 2 to 3 between the two specimens, as shown in Fig. 11b. The reason is the difference between start of bar slippage and its value between the two specimens. In specimen A, the failure of the upper sides of side columns increased after relative deformation of 3.5 and reached the maximum damage at the relative displacement of 4.1. In addition, concrete spalling at cap beam occurred at this relative displacement which is shown in Fig. 12. This caused an increase in the slope of the strength degradation in relative displacement of 3.7 and upper due to the onset of the concrete spalling in side columns.

Figure 12: Damage modes in specimen A, spalling of concrete in side cap beam and middle and right column and rotation of column at relative displacement of 4.1.

Concrete spalling for specimen B occurred at the middle column in relative deformation of about 3 and at the top of the left column and right column in relative displacement of 4. In addition, concrete spalling was observed in the left column at relative deformation of 5.6. This concrete spalling in different relative deformations for the three columns of specimen B increased the slope of the strength degradation from the relative deformation of 4, as is seen in Fig. 11b. In specimen B, the bar slippage occurred after the concrete spalling, and decrease of bond slip and after the degradation strength of 5%. In addition, in the same strength degradation, significant damage was observed in the right column of specimen B and cracking progressed to the concrete core. Overall, the retrofitted specimen (specimen B) showed better behavior compared to the specimen A and the plastic hinge formed well at the middle connection, which is seen in Fig. 13. Moreover, in the right and left connections of the specimen B, where the steel angle with different transverse stress was used, the behavior slightly improved.

Figure 13: Damage modes of specimen B, Fracture of the longitudinal bars of the middle column, complete failure of plastic hinge, bar slippage of the longitudinal bars of the external columns and failure in cap beam of the left connection at relative displacement of 5.6.

The right connection of specimen B with more transverse stress, despite the bar slippage and the crack opening in connection, entered the nonlinear range and flexure plastic hinge formed until the end of loading. The use of pre-stressing caused a delay in damage of cap beam and formed a plastic hinge in the column of the specimen B. Based on the observations made on specimen A, damage progressed in the middle column at the relative deformation of 5. In this relative deformation, the plastic hinge and buckling of the longitudinal bars were observed and the longitudinal bar of the middle column of specimen A fractured. However, no serious damage was observed and the desirable plastic hinge was not formed in the two side columns in specimen A. In addition, the development of undesirable damage such as bar slippage, the opening of the crack in the internal side of cap beam and concrete spalling was observed in the cap beam of specimen A preventing the desirable energy absorption and dissipation. Each damages cause an increase in strength degradation in concrete structures, not seen in specimen B based on Fig.14. In specimen A, slipping of longitudinal bars of the columns also occurred especially in the right column, which resulted in an increase of 10% in strength degradation compared to the specimen B. The results of the numerical model also show the improvement of behavior for the retrofitted specimen.

Due to the improvement of the failure mechanism, the used external longitudinal pre-stressing, which is economical and easy to use, can greatly guarantee the proper behavior of the bridge frame under the seismic loads. As the level of damage in the middle connection is low, the strengthening of this region is not necessary.

Figure 14: Spalling of the external column cap beam at relative displacement of 5.3.

6.3 Stiffness of the specimens

Primary stiffness is an important parameter in designing methods based on displacement and performance, used in current regulations. The initial stiffness of system, K_0, is obtained by dividing the yield force ($F_{y)}$ into its related displacement (Δ_y). The information presented in Table 6 was used for calculation of the initial stiffness of the system for specimens.

The lateral and initial stiffness of the specimens with maximum ductility are shown in Fig. 15. As is seen in Fig. 15, the initial stiffness is calculated somewhat more than the actual value due to the lack of consideration of the pre-loading cracks. Due to the presence of steel angles on both sides of the connection regions of the specimen B, the stiffness for this specimen is higher than that of specimen A. Moreover, the stiffness of the specimen B in the last cycle remains almost constant that indicates that the concrete frame is failed in the last cycle. The lateral stiffness during loading for specimen A, especially in the final cycles, is also greater than the previous non-retrofitted specimen (Bahrani et al., 2017). The numerical model was also able to provide a good approximation of the stiffness of each specimen and the results are presented beside the experimental results.

The sudden drop of curves in figure 15, showing the degradation of stiffness, is due to the use of rubber neoprene bearings between the steel crossbeam and the top of cap beam. The rubber deformation related to cross beam internal deflection was enough large thus the rubber bearing axial loads were approximately the same.

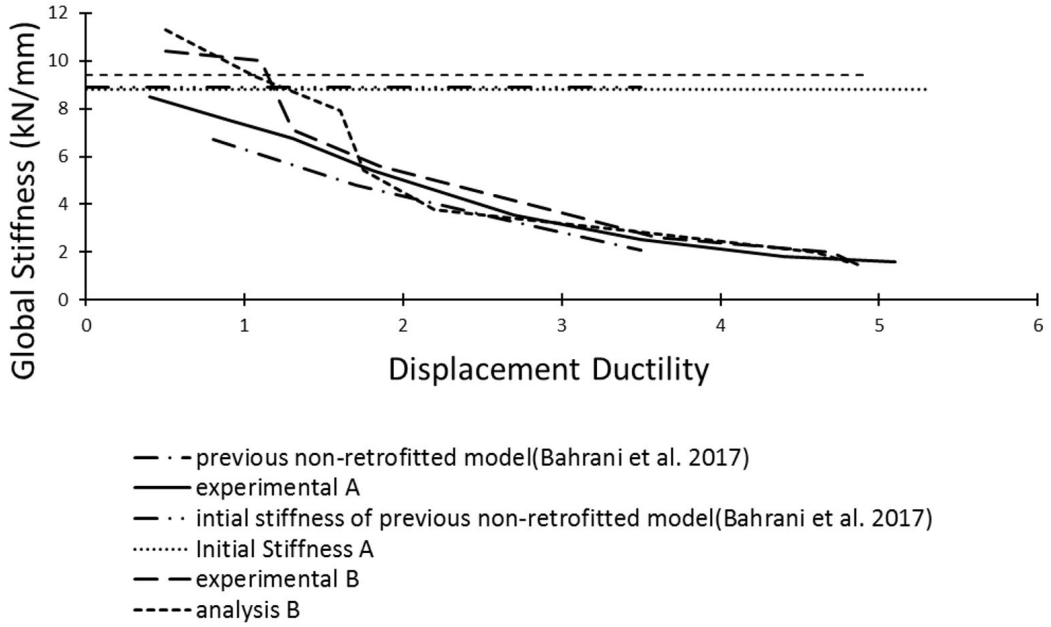

Figure 15: Specimen stiffness to the relative displacement.

Table 6: Mechanical Properties of the Specimens.

Specimen	d_y (mm)	F_y (kN)	K_o (kN/mm)
Previous non-retrofitted Specimen	17	151	8.8
Specimen A	20	175	8.8
Specimen B	21	198	9.4

6.4 Cumulative energy absorption

Fig. 16 shows energy absorption for the specified cycles, increase, and decrease in the energy absorption capacity. Specimen A had modest energy absorption due to defects in design details and the lack of formation of complete plastic hinge; whereas, specimen B had the best energy absorption. Increasing the energy absorption capacity of specimen B improved compared to specimen A, especially in the last cycles. Due to the success in improving the non-linear behavior of the specimen B, the behavior of the frame changed and its energy absorption increased. The numerical results for specimen B also shows this absorbed energy, so one can conclude that in the 1990s codes, the energy absorption has significantly improved. This improvement was about 140% and 233% for specimen A and B, respectively, compared to the specimens of previous similar studies used for 1980s codes. In terms of the cumulative

energy absorption, the values were 290 kN.m and 210 kN.m for specimen A and B, respectively, which shows retrofitting leading to a growth of about 38% in energy absorption.

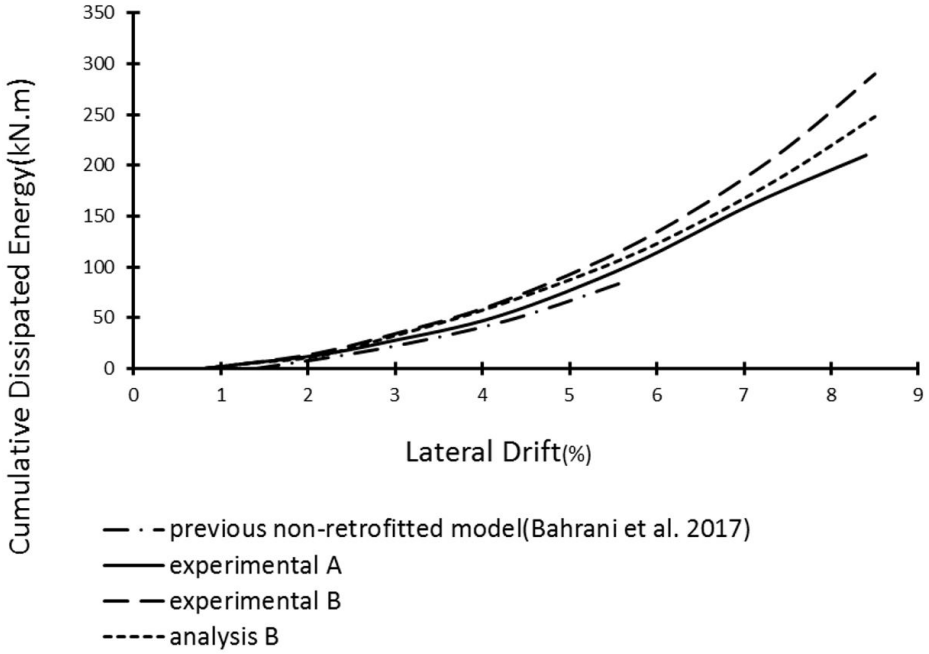

Figure 16: Energy dissipation.

7 CONCLUSION

Two experimental specimens were subjected to cyclic loading for the evaluation of seismic behavior of a two span concrete bridge frame with separate deck, which represents the bridges bent with the even number of spans. A numerical model was used to validate the results using the OpenSsees software as well. According to the previous studies, the need for an accurate evaluation of the frame's behavior is felt with respect to the improved design and implementation details mentioned in 1990s codes compared to the previous ones. Hence, the specimens designed based on newer codes as well as a retrofitted specimen with external pre-stressing were taken in to consideration. A summary of the results of this study is listed in the following:

1. Results showed that the specimen designed with 1990s codes had better seismic behavior compared to specimens designed with older codes, the main reasons for which are the increase of transverse stirrups and the better confinement of concrete in connection region. However, in some aspects, such as ductility, the need for retrofitting is still felt. In addition, rehabilitating of all connections is not necessary for improving frame behavior.
2. The idea of retrofitting specimen for controlling damage in the connection region was successful and was effective in improving the performance of the cap-beams and improving the overall performance of the frame. This strengthening also increased the ductility, absorption and dissipation of energy.
3. Hysteresis curve of specimen A showed a high in-cycle and low out-cycle strength degradation by entering the nonlinear range, whereas for specimen B, the strength degradation occurred with a gentle and desirable trend. The behavior of the specimen B was improved by reducing the bar slippage.
4. In specimen A, plastic hinge did not form at the side columns, whereas in the specimen B, due to the retrofitting, a proper pattern of failure was observed and the plastic hinges were formed in the columns and below the connection regions at high drifts.
5. The predicted initial stiffness for specimen A and related specimen in the previous study were similar, whereas the lateral stiffness during the test especially in the final cycles was much higher for specimen A. For specimen B, an increase in yield force and lateral stiffness was observed in the experiment that is consistent with the numerical model results.

6. The value of energy dissipation in the specimen B increased by 38% compared to specimen A. The energy dissipation in the specimen A, designed based on the 1990s codes, was significantly higher (about 140%) than the same specimen designed by 1980s codes in previous study.
7. The external longitudinal pre-stressing is economical and guarantees the suitable behavior of the concrete bents of bridges.

Acknowledgment:

The experimental part of this paper was sponsored by the International Institute of Earthquake Engineering and Seismology (IIEES) under Project 7515.

Author's Contributions: Conceptualization, MK Bahrani, A Nooralizadeh; Methodology, A Nooralizadeh, N Usefi and MK Bahrani; Investigation, MK Bahrani, A Nooralizadeh, M Zargaran; Writing - original draft, A Nooralizadeh, N Usefi; Writing - review & editing, MK Bahrani, A Nooralizadeh, N Usefi; Funding acquisition, A Nooralizadeh; Supervision, MK Bahrani.

Editor: Pablo Andrés Muñoz Rojas

References

AASHTO. (2007). AASHTO movable highway bridge design specifications, Washington, DC.

Abe, M., and Shimamura, M. (2012). Performance of railway bridges during the 2011 Tōhoku Earthquake. J. Perform. Constr. Facil., 10.1061/(ASCE)CF.1943-5509.0000379, 13–23.

Ahmadi, R., Rashidian, O., Abbasnia, R., Mohajeri Nav, F., Usefi, N. (2016), Experimental and numerical evaluation of progressive collapse behavior in scaled RC beam-column subassemblage, Shock and Vibration.

Architectural Institute of Japan (AIJ). (1994). Structural Design Guidelines for Reinforced Concrete Buildings. Architectural Institute of Japan, Tokyo.

ATC (Applied Technology Council). (1992). Guidelines for cyclic seismic testing of components of steel structures for buildings. Rep. No. ATC- 24, Redwood City, CA.

ATC (Applied Technology Council). (1996). Seismic evaluation and retrofit of concrete buildings. Rep. ATC-40, Redwood City, CA

Bahrani, M.K., Vasseghi, A., Nooralizadeh, A., and Zargaran, M (2017). Experimental and Analytical Study on the Proposed Retrofit Method for concrete Bent in Ordinary Highway Bridges in Iran, J. Bridge Eng., -1—1, DOI: 10.1061/(ASCE)BE.1943-5592.0001045.

Billah, A.H.M., Shahria Alam, M., and Rahman Bhuiyan, M.A. (2012), Fragility analysis of retrofitted multicolumn bridge bent subjected to near-fault and far-field ground motion. Journal of Bridge Engineering 18, no. 10: 992-1004.

Chen, G., Anderson, N., Luna, R., Stephenson, R., El-Engebawy, M., Silva, P., & Zoughi, R. (2005). Earthquake hazards assessment and mitigation: a pilot study in the new madrid seismic zone. *FHWA Report*.

Dodd, L., and Restrepo-Posada, J. (1995). Model for predicting cyclic behaviour of reinforcing steel. J. Struct. Eng., 10.1061/(ASCE)0733 -9445(1995)121:3(433), 433–445.

Fakharifar, M., Chen, G., Dalvand, A., & Shamsabadi, A. (2015). Collapse vulnerability and fragility analysis of substandard RC bridges rehabilitated with different repair jackets under post-mainshock cascading events. International Journal of Concrete Structures and Materials, 9(3), 345-367.

Flores, L. M. (2004). Performance of existing reinforced concrete columns under bidirectional shear and axial loading. Research Rep., Univ. of California, Berkley, CA.

Han, Q., Qin, L., and Wang, P. (2013). Seismic failure of typical curved RC bridges in Wenchuan Earthquake. Proc., 6th China–Japan–US Trilateral Symposium on Lifeline Earthquake Engineering, ASCE, Reston, VA, 425–432.

Hawkins, N.M., Lin, I., and Ueda, T. (1987), Anchorage of reinforcing bars for seismic forces. ACI Structural Journal; 84(5):407–418.

Hosseini, S.M., Mashiri, F., Mirza, O., (2019a). Fatigue Assessment in Steel-Concrete Composite Structure Utilising Blind Bolt Shear Connector, 13th International Conference on the Mechanical Behaviour of Materials (ICM13), 11-14 June, Melbourne, Australia.

Hosseini, S.M., Mashiri, F., Mirza, O., (2019b). Mechanical performance of composite Steel-concrete beams utilising demountable ser connectors, 9th International Conference on Steel and Aluminium Structures (ICSAS19), Bradford, UK, 3-5, July.

Hsu, Y., and Fu, C. (2004). Seismic effect on highway bridges in Chi Chi Earthquake. J. Perform. Constr. Facil., 10.1061/(ASCE)0887 -3828(2004)18:1(47), 47–53.

Javidan, M.M., Kim, J., (2019a), Seismic retrofit of soft-first story structures using rotational friction dampers, journal of structural engineering, In Press.

Javidan, M.M, Kim, J. (2019b). Variance-based global sensitivity analysis for fuzzy random structural systems. Computer-Aided Civil and Infrastructure Engineering. 2019; 34 (7): 602– 615. https://doi.org/10.1111/mice.12436

Javidan, M.M., Kang, H., Isobe, D., Kim, J. (2018). Computationally efficient framework for probabilistic collapse analysis of structures under extreme actions, Engineering Structures, Volume 172, 1 October 2018, Pages 440-452.

Kitayama, K., Otani, S., and Aoyama, H. (1991). Development for Design Criteria for RC Interior Beam-Column Joints. Design of Beam-Column Joints for Seismic Resistance, SP 123-4, 1991. Ed. J. O. Jirsa. ACI.

Kwon, O., Elnashai, A. S., Gencturk, B., Kim, S., Jeong, S., and Dukes, J. (2011), Assessment of seismic performance of structures in 2010 Chile Earthquake through field investigation and case studies. Proc., Structures Congress, ASCE, Reston, VA.

Liu, K.Y., Witarto, W., and Chang, K.C. (2014), Composed analytical models for seismic assessment of reinforced concrete bridge columns, Earthquake Engineering and structural dynamics, DOI: 10.1002/eqe.2470.

Lowes, N.l, Mitra,N., Altoontash, A. (2004). A Beam-Column Joint Model for Simulating the Earthquake Response of Reinforced Concrete Frames. Pacific Earthquake Engineering Research Center, University of California, Berkeley.

Mander, J., Priestley, M., and Park, R. (1988). Theoretical stress–strain model for confined concrete. J. Struct. Eng., 10.1061/(ASCE)0733 -9445(1988)114:8(1804), 1804–1826.

Mohajeri Nav, F., Usefi, N., Abbasnia, R. (2018). Analytical investigation of reinforced concrete frames under middle column removal scenario. Advances in Structural Engineering, 21(9), 1388–1401.

Morita, A., Kaku, T. (1984), Slippage of reinforcement in beam-column joint of reinforced concrete frame. Proceedings of 8th World Conference on Earthquake Engineering. San Francisco; 6:477–484.

Motaref, S., Saiidi, M., and Sanders, D. (2014). Shake table studies of energy- dissipating segmental bridge columns. J. Bridge Eng., 10.1061/(ASCE)BE.1943-5592.0000518, 186–189.

Naito, C.J., Moehle, J.P., Mosalam, K.M. (2001), Experimental and Computational Evaluation of Reinforced Concrete Bridge Beam-Column Connections for Seismic Performance, Berkeley: Pacific Earthquake Engineering Research Center, 2001.

New Zealand Standard 3101 (NZS 1982) — Code Practice for the Design of Concrete Structures.

New Zealand Standard 3101 (NZS 1995) — Code Practice for the Design of Concrete Structures

Noorsuhada, M.N., Soffian Noor, M.S., Muhammad Zakaria M., Azmi I., Jalilluddin A.M., Aqil, Syafeeq T., Kay Dora A.G. (2017). Structural Health Monitoring Of Reinforced Concrete Beam-Column Joint Using Acoustic Emission Technique, International Journal of Advances in Science Engineering and Technology, 5 (3), 50-55.

Otani, S., Sozen, M.A,(1972), Behavior of Multistory Reinforced Concrete Frames during Earthquakes. Structural Research Series No.392, University of Illinois: Urbana.

Pochanart, S., and Harmon, T. (1989) Bond-slip model for generalized excitations including fatigue. ACI Materials Journal; 86(5):465–474.33.

Priestley, M. J. N., Seible, F., and Anderson, D. L. (1993). Proof test of a retrofit concept for the San Francisco double-deck viaducts. Part 1: Design concept, details, and model. Struct. J., 90(5), 467–479.

Priestley,M. J. N., and Paulay, T. (1992). Seismic design of reinforced concrete and masonry buildings, John Wiley and Sons, New York.

Priestley,M. N., Seible, F., and Calvi, G. M. (1996). Seismic design and retrofit of bridges, John Wiley and Sons, New York.

Saatcioglu, M., Alsiwat, J.M., and Ozcebe, G. (1992), Hysteretic behavior of anchorage slip in R/C members. Journal of Structural Engineering, ASCE 1992; 118(9):2439–2458.

Sezen, H., and Moehle, J.P. (2003) Bond-slip behavior of reinforced concrete members. Proceedings of FIB Symposium on Concrete Structures in Seismic Region, CEB-FIP. Athens, Greece.

Shayanfar, MA., Javidan, MM. (2017). Progressive Collapse-Resisting Mechanisms and Robustness of RC Frame–Shear Wall Structures, Journal of Performance of Constructed Facilities, 31(5), 31(5),

Soroushian, P., and Choi, K.B. (1989), Local bond of deformed bars with different diameters in confined concrete. ACI Structural Journal; 86(2):217–222.

Sritharan, S. S., Priestley, M. J. N., and Seible, F. (1999). Enhancing seismic performance of bridge cap beam-to-column joints using prestressing. PCI J., 44(4), 74–91.

Sritharan, S., Priestley, M., and Seible, F. (2001), Seismic design and experimental verification of concrete multiple column bridge bents, ACI Structural Journal, V. 98, No. 3, May-June.

Tehrani, P., Mitchell, D. (2013), Seismic Response of Bridges Subjected to Different Earthquake Types Using IDA, Journal of earthquake engineering, Volume 17, Issue 3.

U.S.: California Department of Transportation (Caltrans 1994) — Bridge Design Specification

United States (U.S.): ACI 352 (1983) — ASCE-ACI Joint Committee.

Untrauer, R. E., and Henry, R.L. (1965), Influence of normal pressure on bond strength. In Journal Proceedings, vol. 62, no. 5, pp. 577-586.

Usefi, N., Sharafi, P., Ronagh, H., (2019). Numerical models for lateral behaviour analysis of cold-formed steel framed walls: State of the art, evaluation and challenges, Volume 138, May 2019, Pages 252-285

Vosooghi, A., and Saiidi, M., (2013). Design guidelines for rapid repair of earthquake-damaged circular RC bridge columns using CFRP. J. Bridge Eng., 10.1061/(ASCE)BE.1943-5592.0000426, 826–836.

Zadeh, M. S., and Saiidi, M. S. (2007). Pre-test analytical studies of NEESR-SG 4-span bridge model using OpenSees. Rep. No. CCEER- 07-3, Civil Engineering Dept., Univ. of Nevada, Reno, NV.

Zhao, J., and Sritharan, S. (2007). Modeling of strain penetration effects in fiber-based analysis of reinforced concrete structures. ACI Struct. J., 104(2), 133.